

Extension of the hcp-fcc ^4He Phase Diagram to about 9 kbar

J. P. Franck^(a) and W. B. Daniels

Department of Physics, University of Delaware, Newark, Delaware 19711

(Received 9 November 1979)

The hcp-fcc transition in ^4He was investigated from 4 to 8.69 kbar by an optical method. The temperature hysteresis increases from 1 to 2.8 K, and the temperature width of the transition from 100 mK to about 2 K. The estimated equilibrium phase-transition line deviates increasingly with higher pressures from theoretical predictions.

Theoretical estimates¹⁻⁴ of the relative stability of the two close-packed phases of ^4He (hexagonal close-packed, and face-centered cubic) have in common that the fcc phase is favored both at high temperatures due to its larger entropy, and at high pressures (i.e., densities) due to a lower static lattice energy. In the most detailed calculations, those of Holian *et al.*,⁴ these tendencies show themselves in the (P, T) plane as a phase-transition line with gradually increasing curvature, leading eventually to negative slope and a maximum pressure for the hcp phase at 0 K. This maximum pressure is estimated to lie in the range 15 to 80 kbar. The present investigation was undertaken to test these predictions to as high pressures as could be achieved. Previous investigations,^{5,6} with use of thermal analysis, could not be extended beyond 4 kbar due to the rapidly increasing width of the transition and the rising background heat capacity, leading to increasingly faint signatures of the transition. It was therefore decided to use an optical method to detect the phase transition. This method makes use of the optical birefringence of the hcp phase as opposed to the optical isotropy of the fcc phase; it was first used at lower pressures by Vos *et al.*⁷

In the present work we report results on the phase transition up to a pressure of 8.69 kbar, corresponding to a molar volume of $7.83 \text{ cm}^3/\text{mole}$. It is found that the phase-transition line appears to continue with constant slope to the highest density investigated, leading to increasingly serious disagreement with the calculations of Holian *et al.*⁴ More detailed kinetic studies of the transition, made possible by the optical method, give further evidence for the martensitic character of the transition.⁸

The crystals were contained in a high-pressure cell made from beryllium copper and sealed with two sapphire windows. The helium space was 4.76 mm in diameter and 13 mm long. The clear optical aperture was 1.59 mm. Helium of research grade (Linde ultrahigh purity, 99.999% ^4He) was used. The crystals were frozen by low-

ering the temperature while keeping the pressure capillary open with a heater (i.e., at constant pressure). Occasionally crystals were also frozen with a blocked capillary, i.e., at constant volume. The optical-detection system utilizes helium-neon laser radiation from a Spectraphysics 145P laser,⁹ which traverses the cell. The ingoing plane of polarization can be adjusted with a polarization rotator. The optical path consists of two room-temperature windows in the cryostat (glass), the two sapphire cell windows, and the helium crystal. Because of stress birefringence in the sapphire windows, as well as the birefringence of the helium crystal (in its hcp phase), the outgoing radiation is elliptically polarized. The phase transition from the hcp to the fcc ^4He phase corresponds then to the removal of a retardation plate from this system. The amount of the retardation and the axis orientation depend on the orientation between c axis and the laser beam direction. The best signal-to-noise ratio was usually obtained in the following way: The cell was cooled to well below the phase transition so that the helium crystal was in its hcp phase. The ingoing plane of polarization was then adjusted until the outgoing elliptically polarized light had minimum eccentricity (i.e., maximum axis ratio b/a). Once this setting had been obtained, a $\lambda/4$ plate followed by a polarizer was used to obtain extinction. When the transition to the fcc phase occurs the retardation plate representing hcp ^4He is removed, and the $\lambda/4$ plate and analyzer combination will pass a certain amount of radiation. The radiation was detected by a Spectraphysics model 404 power meter and monitored on a strip-chart recorder, together with the temperature of the cell.

In Fig. 1 we show a cooling and a heating transition in a crystal of molar volume $V = 7.83 \text{ cm}^3/\text{mole}$. Data that were used for the establishment of the phase diagram were always taken after the crystal had been taken repeatedly through the heating and cooling transition. Heating and cooling rates used for these points were chosen suffi-

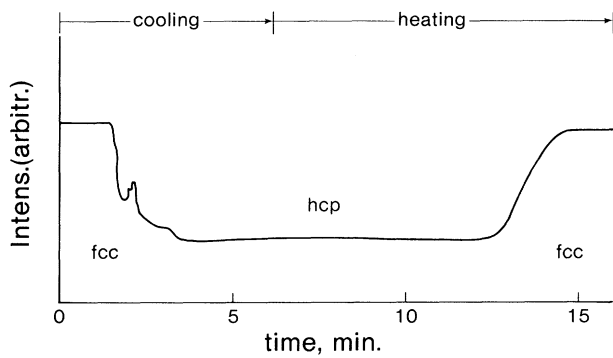


FIG. 1. Optical signature of the transition in a crystal of molar volume $7.83 \text{ cm}^3/\text{mole}$. The average transition pressure is 8.69 kbar. The cooling rate at the fcc-hcp transition is 2.4 K/min and the heating rate at the hcp-fcc transition is 1.1 K/min.

ciently small to eliminate errors due to thermal nonequilibrium between thermometer and helium crystal; the rates did not exceed 50 mK/min. The temperature at which the transition starts in heating is denoted T_h , the temperature at which the cooling transition starts is denoted T_c . Either transition proceeds over a finite temperature interval, the temperature width of the transition. It was found that small changes in T_h and T_c , of up to 100 mK, were taking place when repeatedly traversing the transition. These changes occurred particularly after prolonged heat treatment in one or the other phase. It was also observed that crystal quality influenced these temperatures, although predominantly the cooling transition temperature T_c . An extreme example of this was observed at a molar volume of $V = 8.26 \text{ cm}^3/\text{mole}$ (transition pressure $P = 6943$ bars). This particular crystal had been grown very fast (approximately 1 min) at constant volume and showed poor light transmission. In general, however, the T_c temperatures show no more than 200 mK deviation from a common curve, including crystals that were grown both at constant pressure and constant volume. The scatter of the heating transition temperatures is somewhat less.

In order to obtain the density of the crystal and the transition pressure, we observed the melting point of the crystal, T_m . Melting showed itself as a small decrease in transmitted intensity, which becomes much more pronounced during the melting interval. From the melting point T_m , we obtained the melting pressure P_m using the melting curve of Crawford and Daniels.¹⁰ Isochoric

TABLE I. Transition data, hcp $^4\text{He} \rightarrow$ fcc ^4He .

T_m (K)	V (cm^3/mole)	T_c (K)	T_h (K)	\bar{P}_{tr} ^b (bars)
34.37 ^a	9.44	18.98	20.09	3882
35.16	9.37	19.26	20.35	4017
40.08	8.92	20.36	21.78	4898
45.26	8.58	22.20	23.99	5893
49.12	8.34	22.94	25.02	6665
50.42	8.26	22.81	25.85	6943
50.56	8.25	23.82	25.78	6960
55.07	8.00	24.87	27.45	7943
56.43	7.93	25.68	28.19	8243
58.43	7.83	26.23	29.01	8687

^aThermal analysis.

^bPressure corresponds to $(T_c + T_h)/2$.

pressure corrections between the melting point and the transition temperatures were made with use of the equation-of-state calculations of Spain and Segall.¹¹

In Table I we show the results for the transition temperatures T_c and T_h and the average transition pressure \bar{P}_{tr} for each crystal. Included in the table is also a point taken by use of the thermal analysis method, but not included in previous publications. All crystals studied are identified by their melting temperature. Uncertainties in transition pressure arise predominantly from uncertainties in the determination of T_m ; they are estimated to be about ± 150 bars. The molar volumes given in Table I were also obtained from the equation of state of Spain and Segall¹¹ and they vary from 9.44 to 7.83 cm^3/mole for the present investigation. This corresponds to nearest-neighbor distances in the range 2.81 to 2.63 Å. These values can be compared with the minimum position r_{min} and the "hard-core" diameter σ of the interatomic potential of helium. In the Beck¹² potential these are given by $r_{min} = 2.969$ Å and $\sigma = 2.637$ Å. It appears therefore that at our highest pressure the helium was compressed to about a nearest-neighbor distance equal to σ . The temperature hysteresis, defined as $\Delta T = T_h - T_c$, increases from about 1 K near 4 kbar to about 2.8 K near 9 kbar. The temperature width of the transition also increases with increasing density, from about 100 mK near 4 kbar to about 2 K near 9 kbar.

In Fig. 2 we show the phase diagram in the (P, T) plane. For continuity we have included points taken below 4 kbar by the thermal analysis meth-

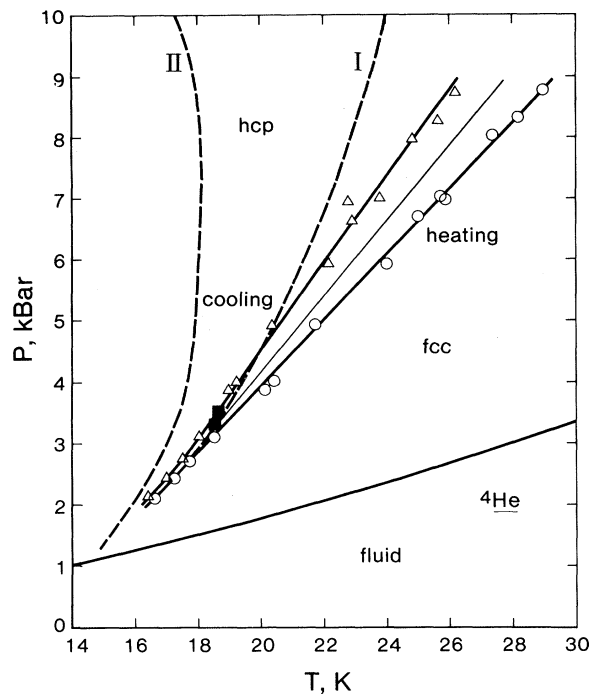


FIG. 2. Phase diagram of ^4He . Open circles, heating transition temperature T_h ; open triangles, cooling transition temperature T_c ; solid squares, hcp and fcc mixed phase, Ref. 13, x rays; light line, possible equilibrium transition line, given by $\frac{1}{2}(T_h + T_c)$, slope 622 bars/K; dashed lines I and II, theoretical estimates from Ref. 4.

od,⁵ excluding only the region near the triple point where anomalous behavior is observed.⁶ As can be seen, excellent agreement exists between the two methods. Although the T_c and T_h temperatures depend somewhat on crystal quality, the scatter is sufficiently small to define curves of T_c and T_h as function of pressure; our estimate of these is shown in Fig. 2. It is remarkable that the line for the transition in heating is linear from about 1.7 kbar to about 9 kbar with a slope of 537 bars/K. The cooling transition line shows gradually increasing slope between 1.7 and 2.5 kbar. Above 2.5 kbar, however, the cooling transition follows again a straight line with slope 707 bars/K. The equilibrium transition line, which is defined by the equality of the Gibbs free energy of the two bulk phases, will lie somewhere in between the cooling and heating transition line. If one assumes, as is common practice in the field of martensitic transitions, that the equilibrium transition temperature is given by $\frac{1}{2}(T_c + T_h)$, then the equilibrium line has a constant slope of 622 bars/K from 2.5

kbar to about 9 kbar. Between 2.5 and 1.7 kbar the slope decreases somewhat, due to the decreasing slope of the cooling transition line, to about 550 bars/K. It is, however, somewhat dubious whether the decrease in slope between 1.7 and 2.5 kbar and the following increase to 622 bars/K is, in fact, a property of the true equilibrium line. As can be seen, such a change in slope is not present in the heating transition line; it is solely brought about by the behavior of the cooling transition line. Since the heating transition is noticeably less sensitive to crystal quality one might be inclined to place the equilibrium line closer to the heating transition. In fact, a straight line can be drawn which at 1.7 kbar is halfway between T_c and T_h , but at higher pressures lies closer to T_c . Such a line has constant slope of 585 bars/K and at 8.5 kbar it is 0.7 K below T_h and 1.4 K above T_c .

Mills and Schuch¹³ reported two crystals in which they observed both the hcp and the fcc phase using x rays for identification. These points are also shown in Fig. 2. According to the description of their experimental procedure, these points probably lie inside the cooling transition range (about 80 mK wide at their pressure) and thus they agree with the present measurements. Their proposed phase line was drawn without knowledge of the temperature hysteresis and is therefore too steep.

In Fig. 2 we also show the two equilibrium lines calculated by Holian *et al.*⁴ The line labeled I is calculated without lattice dynamics corrections to the cell-model internal energy, whereas for the line labeled II these corrections were applied. As can be seen, the experimental data deviate with rising pressure increasingly from these predictions. It is significant that even the cooling transition line lies progressively at higher temperatures than predicted. The disagreement with theory is therefore not very much affected by the difficulties in placing the bulk equilibrium line.

The theoretical phase diagram of Holian *et al.* was obtained by independently calculating the transition temperature, T_{tr} , and the corresponding pressure P_{tr} at various molar volumes. The transition temperature T_{tr} was obtained from

$$T_{tr} = (\Delta H)_{tr} / (\Delta S)_{tr},$$

where the latent heat $(\Delta H)_{tr}$ was obtained as the sum of the zero-point energy difference and static-lattice energy difference. The transition pressure was obtained by differentiation of the internal energy as function of molar volume. As

stated already by Holian *et al.*, the transition pressures are in reasonably good agreement with experiment, so that the disagreement with experiment has to stem from the estimation of the transition temperature. Of the quantities needed to calculate T_{tr} , the transition entropy can be assumed to be known more reliably. The latent heat $(\Delta H)_{tr}$, on the other hand, is more susceptible to small errors in a number of ways. Such errors can arise from the use of incorrect interatomic potentials, the possible importance of three- and four-body interactions, crystal-field effects, and short-range correlations. An account of these various effects has been given by Niebel and Venables.¹⁴

We would like to thank Tom Reed and Tom Reilly for the able and cheerful way in which they provided technical support. One of the authors (J.P.F.) likes to thank the Physics Department and the Unidel Foundation for a very enjoyable stay at the University of Delaware.

This research was supported in part by National Science Foundation Grant No. DMR 78-01-307.

^(a)Permanent address: Department of Physics, Uni-

versity of Alberta, Edmonton, Alta. T6G 2J1, Canada.

¹C. Isenberg and C. Domb, in *Lattice Dynamics*, edited by R. F. Wallis (Pergamon, Oxford, 1965).

²W. G. Hoover, *J. Chem. Phys.* **49**, 1981 (1968).

³B. J. Alder, B. P. Carter, and D. A. Young, *Phys. Rev.* **183**, 831 (1969).

⁴B. L. Holian, W. D. Gwinn, A. C. Luntz, and B. J. Alder, *J. Chem. Phys.* **59**, 5444 (1973).

⁵J. P. Franck, *Phys. Rev. Lett.* **40**, 1272 (1978).

⁶J. P. Franck, *Chem. Phys. Lett.* **63**, 100 (1979).

⁷J. E. Vos, B. S. Blaisse, D. A. E. Boon, W. J. van Scherpenzeel, and R. Kingma, *Physica (Utrecht)* **37**, 51 (1967); J. E. Vos, R. V. Kingma, F. J. van der Gaag, and B. S. Blaisse, *Phys. Lett.* **24A**, 738 (1967).

⁸J. P. Franck, in *Proceedings of the International Conference on Martensitic Transformations*, Cambridge, Massachusetts, 1979 (to be published).

⁹Spectra-Physics, Mountain View, Cal.

¹⁰R. K. Crawford and W. B. Daniels, *J. Chem. Phys.* **55**, 5651 (1971).

¹¹I. L. Spain and S. Segall, *Cryogenics* **11**, 26 (1971).

¹²D. E. Beck, *Mol. Phys.* **14**, 311 (1968), and **15**, 332 (1968).

¹³R. L. Mills and A. F. Schuch, *J. Low Temp. Phys.* **16**, 305 (1974).

¹⁴K. F. Niebel and J. A. Venables, in *Rare Gas Solids*, edited by M. L. Klein and J. A. Venables (Academic, London, 1976), Vol. I.

Structure of Defect Cascades in Fast-Neutron-Irradiated Aluminum by Diffuse X-Ray Scattering

B. v. Guérard, D. Grasse, and J. Peisl

Sektion Physik, Universität München, 8 München 22, Germany

(Received 14 May 1979)

We measure diffuse x-ray scattering close to Bragg reflections in aluminum single crystals after irradiation with fast-reactor neutrons at 4.6 K. Detailed evaluation of the results for low irradiation dose demonstrates that defects are located in cascades (radius $r_K \approx 50$ Å; defect number, $Z_K \approx 200$). Within a cascade the defects form agglomerates ($r_A \approx 5$ Å, $Z_A \approx 3$). For irradiation doses $> 2.4 \times 10^{18}$ n/cm² the cascades partly overlap.

Irradiation of solids with fast heavy particles produces vacancies and interstitials (Frenkel pairs) in displacement cascades. The actual defect concentration and correlation within a cascade depend on the specific properties of the material and the irradiation conditions. Computer simulations¹⁻³ predict a cascade structure with a high-vacancy concentration (depleted zone) surrounded by a cloud of interstitials.⁴ A detailed understanding of the defect correlation in displacement cascades is of special interest as it strongly influences the formation of large defect agglomerates during thermal annealing after low-temperature irradiation or during irra-

diation at elevated temperatures. Thermally stable defect agglomerates are the central problem of reactor materials.

In this Letter we report measurements of the diffuse x-ray scattering close to Bragg reflections [Huang diffuse scattering (HDS)] from low-temperature neutron-irradiated Al crystals. This method has been used successfully to determine the symmetry and strength of point defects and to study the formation of defect clusters.⁵⁻⁸

We are able for the first time to detect a modification of the HDS close to the Bragg peak due to a nonrandom defect distribution. This gives detailed information on the defect distribution in